Direct intratumoral infusion of liposome encapsulated rhenium radionuclides for cancer therapy: Effects of nonuniform intratumoral dose distribution

Brian A. Hrycushko, Shihong Li, and Beth Goins
Department of Radiology, University of Texas Health Science Center at San Antonio, San Antonio, Texas 78229

Randal A. Otto
Department of Otolaryngology-Head and Neck Surgery, University of Texas Health Science Center at San Antonio, San Antonio, Texas 78229

Ande Bao[a)]
Department of Radiology, University of Texas Health Science Center at San Antonio, San Antonio, Texas 78229 and Department of Otolaryngology-Head and Neck Surgery, University of Texas Health Science Center at San Antonio, San Antonio, Texas 78229

(Received 18 October 2010; revised 17 December 2010; accepted for publication 17 January 2011; published 16 February 2011)

Purpose: Focused radiation therapy by direct intratumoral infusion of lipid nanoparticle (liposome)-carried beta-emitting radionuclides has shown promising results in animal model studies; however, little is known about the impact the intratumoral liposomal radionuclide distribution may have on tumor control. The primary objective of this work was to investigate the effects the intratumoral absorbed dose distributions from this cancer therapy modality have on tumor control and treatment planning by combining dosimetric and radiobiological modeling with *in vivo* imaging data.

Methods: ^{99m}Tc-encapsulated liposomes were intratumorally infused with a single injection location to human head and neck squamous cell carcinoma xenografts in nude rats. High resolution *in vivo* planar imaging was performed at various time points for quantifying intratumoral retention following infusion. The intratumoral liposomal radioactivity distribution was obtained from 1 mm resolution pinhole collimator SPECT imaging coregistered with CT imaging of excised tumors at 20 h postinfusion. Coregistered images were used for intratumoral dosimetric and radiobiological modeling at a voxel level following extrapolation to the therapeutic analogs, ^{186}Re/^{188}Re liposomes. Effective uniform dose (EUD) and tumor control probability (TCP) were used to assess therapy effectiveness and possible methods of improving upon tumor control with this radiation therapy modality.

Results: Dosimetric analysis showed that average tumor absorbed doses of 8.6 Gy/MBq (318.2 Gy/mCi) and 5.7 Gy/MBq (209.1 Gy/mCi) could be delivered with this protocol of radiation delivery for ^{186}Re/^{188}Re liposomes, respectively, and 37–92 MBq (1–2.5 mCi)/g tumor administered activity; however, large intratumoral absorbed dose heterogeneity, as seen in dose-volume histograms, resulted in insignificant values of EUD and TCP for achieving tumor control. It is indicated that the use of liposomes encapsulating radionuclides with higher energy beta emissions, dose escalation through increased specific activity, and increasing the number of direct tumor infusion sites improve tumor control. For larger tumors, the use of multiple infusion locations was modeled to be much more efficient, in terms of activity usage, at improving EUD and TCP to achieve a tumoricidal effect.

Conclusions: Direct intratumoral infusion of beta-emitting radionuclide encapsulated liposomes shows promise for cancer therapy by achieving large focally delivered tumor doses. However, the results of this work also indicate that average tumor dose may underestimate tumoricidal effect due to substantial heterogeneity in intratumoral liposomal radionuclide distributions. The resulting intratumoral distribution of liposomes following infusion should be taken into account in treatment planning and evaluation in a clinical setting for an optimal cancer therapy. [DOI: 10.1118/1.3552923]

Key words: radionuclide therapy, liposome, intratumoral, dosimetry, head and neck cancer

I. INTRODUCTION

The ultimate goal in cancer therapy is complete tumor eradication with minimal damage to healthy organs or tissue. With radiation therapy, tumor control is considered a probabilistic event where higher absorbed doses improve upon tumor control. This places the radiation oncologist with the important

task of delivering sufficient absorbed dose for attaining complete tumor eradication while not delivering so much absorbed dose as to bring about unacceptable normal tissue toxicity. Technological innovations have improved radiation delivery, thus providing for higher absorbed dose to be given to tumors while reducing absorbed dose to normal tissues. Focused radiation therapy with beta-emitting radionuclides has the potential to further improve therapeutic effectiveness by achieving ablative tumor doses with minimal dose delivered to surrounding normal tissue. This is due to the sharp drop-off in dose with distance as seen in beta-emitting radionuclide dose point kernels (DPKs).[1–4] Although encouraging results have been seen in the clinical setting,[5,6] maximized potential has yet to be achieved. A benefit of treating with beta emitters is that cellular uptake is not a requirement for tumoricidal effect, as is common in many antitumor drugs, and cells several millimeters away from the liposomal radionuclides receive considerable cross-fire absorbed dose. In rabbit sarcomas, it has been observed that intravenously administered liposomes, on average, had a maximum percent tumor volume coverage of 72% at 48 h postinjection.[7] This incomplete tumor volume uptake with antitumor drug encapsulated liposomes may be ineffective for tumor control if individual tumor cells cannot absorb the drug; however, this may be overcome by the locoregional treatment resulting from liposome encapsulated beta-emitting radionuclides.

Two factors possibly responsible for diminishing the tumoricidal effect, thus resulting in a varied clinical response with radionuclide therapy, include (1) nonuniform intratumoral absorbed dose distributions resulting from heterogeneous radionuclide uptake patterns and (2) poor tumor-to-normal tissue uptake ratios of therapeutic drugs following systemic administration techniques. The latter can be greatly improved through direct intratumoral delivery and liposomal encapsulation of the therapeutic radionuclides.[8] A therapeutic benefit from intravenously administered radionuclide encapsulated liposomes may be passively achieved by extravasation through abnormal leaky tumor vasculature known as the enhanced permeability and retention effect or actively achieved by targeting of specific cancer cell receptors and angiogenic markers.[9] However, low tumor-to-normal tissue uptake ratios and delayed tumor accumulation observed in animal studies may result in an insufficient amount of activity to be safely administered for achieving a desired tumoricidal effect when translated to a clinical setting.[10] Direct intratumoral infusion increases therapeutic potential compared to systemic delivery methods by directly placing a high concentration of therapeutic radionuclides within the target region without a delayed accumulation. In turn, the dose delivered to bone marrow, the most common dose-limiting tissue for systemically delivered radiopharmaceuticals, as well as other organs is greatly reduced. Using liposomes as radionuclide carriers further increases therapeutic potential by providing improved sustained retention compared to free radionuclide compounds, thus allowing for a much higher absorbed dose to the injected region and a reduction in activity cleared to the body.[11]

Intratumoral absorbed dose distributions have become a popular topic with radionuclide therapy modalities with the increased use of hybrid imaging, and it has become evident that dose heterogeneity can have a considerable impact on tumor control. The commonly used "average tumor dose" may not provide an applicable relationship between treatment and effect, in turn, lessening the ability to predict treatment outcome. This work investigates the effects the intratumoral liposome encapsulated radionuclide distribution following direct intratumoral infusion may have on tumor control. This is accomplished through high resolution *in vivo* imaging of the intratumoral distribution of ^{99m}Tc liposomes in a small animal xenograft tumor model and extrapolating to therapeutic analogs, ^{186}Re/^{188}Re liposomes, which have a similar *in vivo* behavior due to their similar chemistry and the same mechanism of liposome encapsulation.[8,12–15] Analysis included dosimetric and radiobiological index modeling commonly used in radiation therapy for prediction of tumor response and therapy assessment. With this treatment design, possible methods of improving upon tumor response through the use of ^{188}Re radionuclides, which emit beta particles with higher energy (^{186}Re: E_{avg}=0.329 MeV and CSDA range =0.483 g/cm^2; and ^{188}Re: E_{avg}=0.795 MeV and CSDA range=1.046 g/cm^2), increased specific activity, and multisite direct intratumoral infusion are discussed.[16] To our knowledge, this is the first study that attempts to correlate *in vivo* intratumoral liposome distributions following direct intratumoral infusion with modeled therapy response.

II. METHODS AND MATERIALS

II.A. Head and neck squamous cell carcinoma (HNSCC) xenografts in nude rats

Animal experiments were conducted in accordance with the NIH Animal Use Guidelines and were approved by the University of Texas Health Science Center at San Antonio (UTHSCSA) Institutional Animal Care Committee. Animals were anesthetized with 1%–3% of isoflurane (Vedco, St. Joseph, MO) in 100% oxygen using an anesthesia inhalation device (Bickford, Wales Center, NY).

A human head and neck cancer xenograft model was used in nude rats. SCC-4 cell line (ATCC, Manassas, VA) was cultured as previously described.[17] Male *rnu/rnu* athymic nude rats (Harlan, Indianapolis, IN) at age 4–5 weeks (75–100 g) were inoculated subcutaneously with 5×10^6 SCC-4 tumor cells in 0.2 ml of saline on the dorsum at the level of the scapulae. Tumor size was obtained by measuring the length (l), width (w), and thickness (t) of each tumor with a caliper. Tumor volumes were calculated using an ellipsoid volume formula, $V=(\pi/6)lwd$.[18] This tumor xenograft model has previously been characterized with hematoxylin-eosin (HE) staining and described as showing confluent areas of central necrosis with increased vascularity toward the periphery of the tumor capsule.[17] The HE staining showed the tumor model to be an appropriate HNSCC tumor model for animal studies on HNSCC.

II.B. Liposome preparation and radionuclide encapsulation

Liposome preparation and characterization followed a previously described protocol.[11] The neutral surface charged liposomes used have a lipid formulation comprised of distearoylphosphatidylcholine (Avanti Polar Lipids, Alabaster, AL) and cholesterol (Calbiochem, San Diego, CA) (molar ratio of 55:45). In brief, after sequential extrusion through polycarbonate filters with different pore sizes from 2 μm to 100 nm at 55 °C (Lipex Extruder, Northern Lipids, Vancouver, Canada), the resulted liposomes had 60 mM (36.5 mg/ml) total lipid concentration with a medium of 150 mM sucrose, 200 mM glutathione (GSH), and 300 mM ammonium sulfate (pH 5.1 in sterile water). After extrusion, repeated ultracentrifugation at 41 000 rpm (Ti 50.2 rotor, Beckman, Fullerton, CA) was used to remove unencapsulated GSH. The final liposome pellets were resuspended in 300 mM ammonium sulfate (pH 5.1) containing 300 mM sucrose in sterile water at a total lipid concentration of 60 mM and stored at 4 °C until needed. Liposome particle diameter was measured with a 488 nm DLS laser light scattering instrument equipped with a DynaPro Dynamic Light Scattering system (Wyatt Technology, Santa Barbara, CA) and was found to be 108.0 ± 26.4 nm (mean $\pm$ SD). Endotoxin levels were assayed with limulus amebocyte lysate Pyrotell (Associates of Cape Cod Inc., E. Falmouth, MA) and were less than 12.5 EU/ml. There were no bacteria or fungus growth during the 14 day culture.

Labeling of liposomes with ^{99m}Tc-radionuclides consisted of postloading of ^{99m}Tc-*N*,*N*-bis(2-mercaptoethyl)-*N*′,*N*′-diethyl-ethylenediamine (BMEDA) as previously described.[16] In brief, the preparation of ^{99m}Tc liposomes included two steps: (1) The preparation of ^{99m}Tc-BMEDA mediated by the reduction in ^{99m}Tc-pertechnetate with stannous chloride and with the use of the intermediate ligand, glucoheptonate and (2) postloading of ^{99m}Tc-BMEDA into the liposomes followed by purification of ^{99m}Tc liposomes with Sephadex G-25 column chromatography eluted with PBS (pH 7.4) buffer.

II.C. Image acquisition and analysis

Nude rats (n=4) with average measured tumor volumes of 1.36 ± 0.46 cm^3 were intratumorally infused with a volume of ^{99m}Tc liposomes being 20% of the individual rat tumor volumes. A single infusion location was used with the needle tip placed at a central location of the tumors. The infusion rate was set constant at 0.50 ml/min. Static planar gamma camera images were acquired using a micro-SPECT/CT scanner (XSPECT, GammaMedica, Northridge, CA) using a parallel hole collimator with the rat in the prone position. A standard ^{99m}Tc source with known activity was positioned adjacent to the rat within the field of view (FOV) for image quantification. Images were acquired immediately following infusion, at 4 h, and at 20 h postinfusion. Regions of interest (ROIs) were drawn around tumors and the standard using MANGO imaging software (Research Imaging Institute, UTHSCSA, San Antonio, TX) to quantify radioactivity within each ROI, and first order exponential curves were fit to determine clearance rates for individual rats. After 20 h planar imaging, animals were euthanized by cervical dislocation under deep isoflurane sedation. Tumors were excised for 1 mm pinhole collimator SPECT/CT imaging using the micro-SPECT/CT scanner to determine intratumoral activity distribution. Excised tumors were placed on a foam pad so as to not add artifacts to CT images and for accurate tumor segmentation. SPECT images were acquired with the radius of rotation set as small as possible while keeping each tumor within the FOV during the entire image acquisition. Image acquisitions included 32 projections at 90 s per projection to obtain 64 frames of raw projections from two detectors for tomographic image reconstruction. CT images were acquired (75 kVp, 370 mA, and 256 projections) with tumors maintained at the same position for SPECT/CT image coregistration. Following SPECT/CT imaging, tumors were collected for radioactivity counting using a Wallac 1480 Wizard 3 in. automatic well counter (PerkinElmer Life Sciences, Boston, MA).

SPECT and CT images were input to MATLAB software (ver. 7.4.0.287 [R2007a], MathWorks, Natick, MA) in matrix format with voxel sizes of $0.2 \times 0.2 \times 0.2$ mm^3. The intratumoral activity measured by the well counter was converted from counts/min to decays/min using the efficiency of the well counter and used for normalization purposes with the 20 h postinfusion SPECT images to calculate activity within each voxel. The effective clearance rate, calculated from the curve fitting from planar imaging, was assumed to be the same for every voxel and was used to calculate initial ^{99m}Tc activity in each voxel. It is important to note that this technique, as previously described and used as an alternative to multiple SPECT images, has the implicit assumption that the relative spatial distribution as measured during the SPECT/CT image acquisition remains constant.[19,20] Different regions within the tumor may have variations in clearance rates, the effects of which have previously been investigated for uptake of systemically administered radionuclides; however, intratumoral variation in clearance rates is unknown for direct intratumoral infusion of liposome encapsulated radionuclides.[21] Low intratumoral variation seems probable due to the very slow clearance following the disappearance of the injection convection force after infusion and the fact that lipid nanoparticles, being larger than small molecular radionuclide compounds, have a lower capacity for intratumoral diffusion.

Biological clearance rates were then combined with the physical half lives of ^{186}Re/^{188}Re to extrapolate to effective clearance rates for the therapy analogs. This assumes a similar biological clearance rate and intratumoral distribution for ^{99m}Tc liposomes and ^{186}Re/^{188}Re liposomes. Cumulative activity was then calculated for individual voxels to be used with dose calculations.

II.D. Dosimetry and radiobiological modeling

Table I provides a list of symbol definitions and applicable values used for dosimetric and radiobiological model-

TABLE I. Symbol explanations and values used for simulations.

Symbol	Description	Value (if applicable)
$D(i,j,k)$	Voxel dose	N/A
K	DPK matrix	N/A
$\tilde{A}$	Cumulative activity matrix	N/A
EUD_d	Equivalent uniform dose to target region given in d Gy fractions	N/A
ρ_i	Voxel tumor clonogen density	1.8×10^3 clonogens/cm^3 [a]
v_i	Voxel volume	N/A
α/β	Ratio describing irreparable and reparable mechanisms	15 Gy[b]
α	Relates to initial slope of linear-quadratic model	0.35 Gy^{-1}
β	Relates to downward curvature of linear-quadratic model	0.0233 Gy^{-2}
γ	Repopulation time constant	0.015 days^{-1} [c]
d	Daily dose per fraction	2 Gy
$T_{\mathrm{eff},i}$	Effective treatment time	N/A
$D_{T_{\mathrm{eff},i}}$	Dose delivered in effective treatment time	N/A
$\mathrm{RE}_{T_{\mathrm{eff},i}}$	Relative effectiveness per unit dose	N/A
λ_{ET}	Effective decay constant from tumor	N/A
μ	Repair time constant	5.55 days^{-1} [d]
$\dot{D}_{0,i}$	Initial dose rate of voxel i	N/A
BED_i	Biological effective dose	N/A
TCP_T	Tumor control probability	N/A

[a]Data from in Ref. 31.
[b]Data from Ref. 32.
[c]Data from Ref. 33.
[d]Data from Ref. 34.

ing. The DPK convolution technique, which is based on convolving a radionuclide DPK with a cumulative activity distribution, was used to calculate intratumoral dose distributions.[4,22,23] The EGSnrc Monte Carlo simulation user code EDKnrc was used to generate DPKs, which include both beta and photon emissions of ^{186}Re and ^{188}Re radionuclides, within a water medium.[24–27] The DPKs were input into matrix format in MATLAB with the same voxel dimensions as that of the SPECT/CT images, and the convolution of the DPK matrix with the tumor cumulative activity matrix was calculated using Fourier transform (FT), multiplication $(\cdot)$, followed by inverse Fourier transform (FT^{-1}),[4,23]

$$D(i,j,k)=\mathrm{FT}^{-1}\{\mathrm{FT}[K(i,j,k)]\cdot\mathrm{FT}[\tilde{A}(i,j,k)]\}, \tag{1}$$

where i, j, and k are voxel indices. The calculated absorbed dose distributions were used to assess intratumoral absorbed dose heterogeneity with the use of dose-volume histograms (DVHs).

Effective uniform dose (EUD) and tumor control probability (TCP) were used to assess the radiobiological effects and predict therapy response from the nonuniform intratumoral dose distributions. EUD, defined as the uniform absorbed dose of which produces the same biological outcome as the absorbed dose of which is delivered heterogeneously throughout the tumor,[28] was referenced to external beam radiotherapy (EBRT) delivering a daily fraction of 2.0 Gy within a few minutes for five fractions per week to mimic a conventional EBRT treatment regimen. Assuming the response of the tissue to be the clonogen weighted mean of the voxels, the EUD is determined from the linear-quadratic model and was calculated for each tumor using[28,29]

$$\mathrm{EUD}=\frac{-\ln\left[\frac{\sum_{i=1}^{N}\rho_i v_i\exp(-\alpha\cdot\mathrm{BED}_i)}{\sum_i^N\rho_i v_i}\right]}{\alpha+\beta d-\frac{1.4\gamma}{d}}. \tag{2}$$

For the protracted radiation delivery provided by the liposome encapsulated radionuclides, the biological effective dose (BED) is calculated using[29]

$$\mathrm{BED}_i=D_{T_{\mathrm{eff},i}}\times\mathrm{RE}_{T_{\mathrm{eff},i}}-\frac{\gamma\cdot T_{\mathrm{eff},i}}{\alpha}, \tag{3}$$

$$T_{\mathrm{eff},i}=\frac{1}{\lambda_{\mathrm{ET}}}\ln\left(\frac{\alpha\cdot\dot{D}_{0,i}}{\gamma}\right), \tag{4}$$

$$D_{T_{\mathrm{eff},i}}=D_i[1-\exp(-\lambda_{\mathrm{ET}}\cdot T_{\mathrm{eff},i})], \tag{5}$$

$$\mathrm{RE}_{T_{\mathrm{eff},i}}=1+\left(\frac{\beta}{\alpha}\right)\left[\left(\frac{2\dot{D}_{0,i}\cdot\lambda_{\mathrm{ET}}}{(\mu-\lambda_{\mathrm{ET}})[1-\exp(-\lambda_{\mathrm{ET}}\cdot T_{\mathrm{eff},i})]}\right)\right]\times\left(\frac{1-\exp(-2\lambda_{\mathrm{ET}}\cdot T_{\mathrm{eff},i})}{2\lambda_{\mathrm{ET}}}-\frac{1-\exp[-(\mu+\lambda_{\mathrm{ET}})T_{\mathrm{eff},i}]}{\mu+\lambda_{\mathrm{ET}}}\right). \tag{6}$$

TCP, defined by the Poisson statistics model, is the probability of having no surviving clonogens. It is determined for the tumor by considering the intratumoral absorbed dose heterogeneity using[30]

$$\mathrm{TCP}_i=\exp[-\rho_i v_i\exp(-\alpha\cdot\mathrm{BED}_i)], \tag{7}$$

$$\mathrm{TCP}=\prod_{i=1}^{N}\mathrm{TCP}_i. \tag{8}$$

The *in vivo* animal study used a single tumor infusion location with the needle tip placed at a central location. The delivery protocol may not be optimal as a poor distribution of liposomal radionuclides following infusion can be detrimental to treatment outcome. In this work, it was desired to know how multiple injection locations could possibly affect tumor control. For modeling purposes, it was assumed that the use of multiple tumor infusion locations would improve the activity coverage of the tumor. Multiple injection locations were extrapolated from the single injection location images and simulated by (1) halving the cumulative activity within each voxel for the intratumoral activity distribution resulting from the single infusion location site and (2) dis-

TABLE II. Dosimetric values normalized to the injected activity.

	Average dose per injected activity (Gy/MBq)		Minimum dose per injected activity (Gy/MBq)		Maximum dose per injected activity (Gy/MBq)	
	^{186}Re	^{188}Re	^{186}Re	^{188}Re	^{186}Re	^{188}Re
Rat 1	9.96	6.44	0.001	0.019	91.68	39.53
Rat 2	6.40	4.35	0.001	0.009	55.76	24.40
Rat 3	8.39	4.45	0.002	0.061	51.11	17.45
Rat 4	9.668	7.37	0.008	0.318	99.65	48.36
Average ± SD	8.60 ± 1.62	5.65 ± 1.50	0.003 ± 0.003	0.102 ± 0.146	74.55 ± 24.67	32.44 ± 14.06

tributing that cumulative activity to voxels which received less than the new average cumulative activity per voxel using

$$\tilde{A}_i = \tilde{A}_{i0} + \tilde{A}_{\text{tot}} \times \left[\frac{(\tilde{A}_{\text{avg}} - \tilde{A}_{i0})^2}{\Sigma_{i=1}^{N} (\tilde{A}_{\text{avg}} - \tilde{A}_{i0})^2} \right], \quad (9)$$

where $\tilde{A}_i$ is the final cumulative activity of voxel i after the multiple injections, $\tilde{A}_{i0}$ is the halved cumulative activity in voxel i following step (1) from above, $\tilde{A}_{\text{tot}}$ is the total adjusted cumulative activity to be distributed ($\Sigma_{i=1}^{N} \tilde{A}_{i0}$), and $\tilde{A}_{\text{avg}}$ is the average cumulative activity per voxel within the tumor following step (1) from above. This allocation method preferentially distributes the cumulative activity to voxels with lower initial cumulative activity by weighting with the square of the difference from the average. Following the redistribution of cumulative activity, the total injected activity and cumulative activity are the same as those from the single infusion location used in the animal study. Although there are various algorithms to simulate multiple injection locations, including the actual number of injections, the model used considers the effects of spreading out the intratumoral liposome distribution. Herein, the technique described would follow an injection protocol of a single injection, followed by numerous local injections in regions of low radionuclide concentration to cover the entire tumor more uniformly with radioactive liposomes.

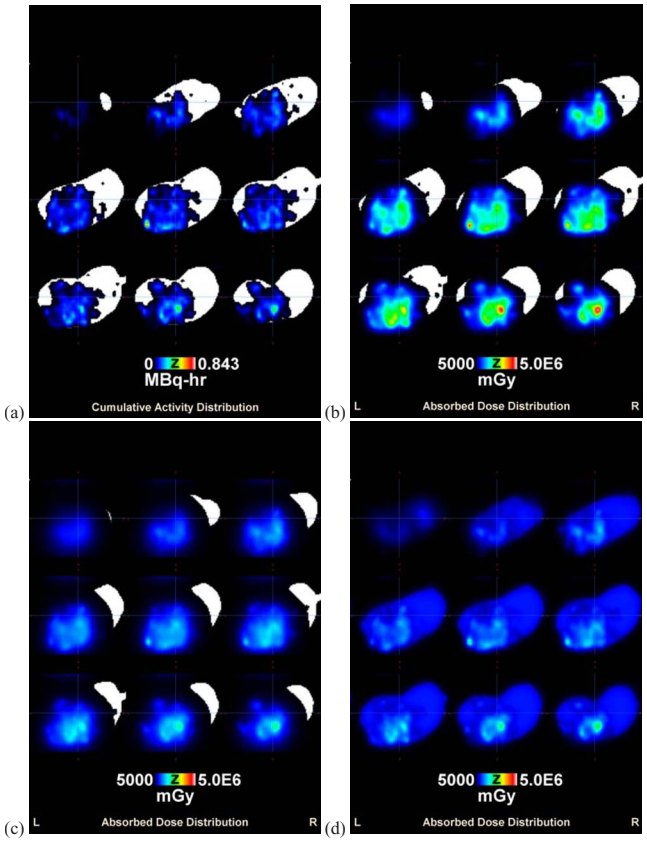

FIG. 1. Intratumoral cumulative activity and absorbed dose distributions overlaid on the binary image of excised tumor showing every third slice. (a) Cumulative activity distribution for ^{186}Re liposomes resulting from the single injection location, (b) resulting ^{186}Re-liposome absorbed dose distribution from the cumulative activity distribution of (a), (c) resulting ^{188}Re-liposome absorbed dose distribution from the same cumulative activity distribution of (a), and (d) resulting ^{186}Re-liposome absorbed dose distribution following the multiple injection location simulation.

III. RESULTS

III.A. Dosimetry

Table II shows the intratumoral dose estimation statistics for individual rats as well as average group values normalized to the injected activity. Although an injected volume equal to 20% of the individual rat tumor volume was used, the absorbed dose depends on the actual specific activity (radioactivity per volume) infused into each tumor. For the protocol used with this animal imaging study, 37–92 MBq (1–2.5 mCi) /g tumor was infused. By normalizing the injected activity, the results can be extrapolated to increase specific activity to a desired amount while keeping the volume injected at 20% of the tumor volume. It is clear that high absorbed doses may be delivered to the tumor for a small amount of injected activity as a result of the sustained retention provided by the liposome encapsulation. A sample intratumoral cumulative activity and resulting absorbed dose distribution overlaid on a binary CT tumor image is shown in Fig. 1 (every third slice shown). Figure 1(a) shows the intratumoral liposome distribution heterogeneity from the single injection location and the resulting absorbed dose from ^{186}Re [Fig. 1(b)] and ^{188}Re [Fig. 1(c)]. Intratumoral absorbed dose distributions are represented in DVHs for ^{186}Re liposomes (a) and ^{188}Re liposomes (b) in Fig. 2. Semilog graphs are used to better illustrate low dose regions. Both Table II and Fig. 2 display a high level of intratumoral absorbed dose heterogeneity with this treatment modality for both radionu-

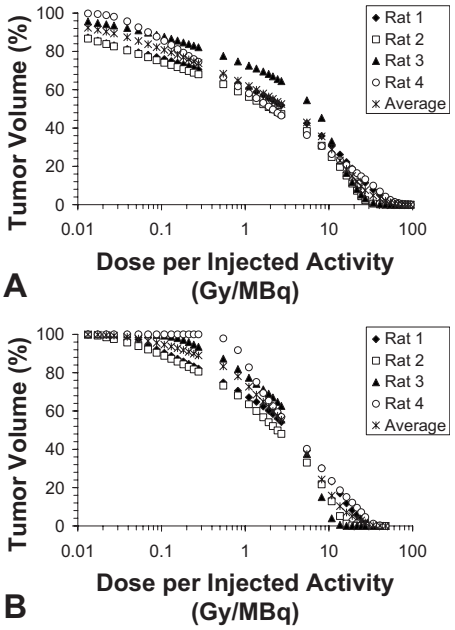

FIG. 2. Average and individual tumor DVHs for ^{186}Re liposomes (a) and ^{188}Re liposomes (b) normalized to the injected activity representing the percentage of tumor volume receiving a specific dose or higher per injected activity.

clides. The higher minimum dose and the improved DVHs for ^{188}Re indicate that higher energy beta emissions can improve tumor absorbed dose coverage.

III.B. Radiobiological modeling

Table IIIa depicts the radiobiological index calculation results following extrapolation of the ^{99m}Tc-liposome infusion data to the therapy counterparts, ^{186}Re/^{188}Re liposomes, as discussed in Sec. II. Although each tumor was shown to receive an extremely high average absorbed dose from this treatment technique, the calculated EUD and TCP values were insufficient for tumor control for most of the tumors. Only rat 4 would have a consequential EUD and TCP for tumor control with ^{188}Re liposomes. This tumor had an intratumoral distribution of liposomes, which delivered a minimum dose of 11.9 Gy (Tables II and III), and again shows that the more energetic beta emissions are able to increase tumor absorbed dose coverage compared to ^{186}Re liposomes.

Table IIIb shows the ^{186}Re/^{188}Re activity, which would have been required to achieve greater than 99% TCP for each rat. This assumes the same infused volume (20% of the tumor volume), but specific activity would be increased. This is achieved in dose simulations by multiplying the cumulative activity by a factor and assuming the increased specific activity would not alter intratumoral liposome distribution or kinetics. It is interesting to note that the required activity to reach 99% TCP was, on average, about 120 and 8 times the injected activity of Table IIIa for ^{186}Re and ^{188}Re, respectively, even for the large average tumor doses of Table IIIa. The much less average required activity from the ^{188}Re liposomes (511 MBq [13 mCi]) compared to ^{186}Re liposomes (8057 MBq [217 mCi]) is due to considerable tumor cross-fire dose from ^{188}Re. Regions within the tumor with low levels of activity are still able to receive a considerable absorbed dose with ^{188}Re liposomes. The results of the ^{186}Re-liposome calculations indicate that simple dose escalation through increased specific activity may not be feasible for tumor control due to the shorter beta penetration of this radionuclide. Poor intratumoral activity coverage from the single infusion site may require extensive increase in the required specific activity for achieving tumor control. On average, about 64×10^3 Gy, an ablative dose level, was calculated to achieve greater than 99% TCP, and the required injected activity (8057 MBq [217 mCi]) may be significant enough to consider toxicity of normal organs/tissues from which there is abundant liposomal uptake (e.g., liver, spleen, and kidneys) due to the longer half-life of ^{186}Re (89.2 h for ^{186}Re and 17.0 h for ^{188}Re).

Table IIIc depicts the radiobiological index calculation results following the extrapolation of the single injection locations used for the *in vivo* animal imaging study to multiple injection locations following the protocol described in Sec. II. Following the redistribution of cumulative activity, the total injected activity and cumulative activity are the same as those from Table IIIa. Figure 1(d) shows a sample absorbed dose distribution following redistribution of the cumulative activity distribution of Fig. 1(a). A much improved absorbed dose coverage is achieved for Fig. 1(d) compared to Fig. 1(b) for the same amount of injected activity. Table IIIc shows that the simulations of multiple injection locations increased EUD and TCP values to tumoricidal levels using the same injected activity for individual tumors as that used for the single injection locations in Table IIIa. The infused activities of Tables IIIa–IIIc indicate that the use of multiple injections is much more efficient in achieving tumor control, in terms of activity usage, than simply increasing the specific activity of ^{186}Re/^{188}Re liposomes. By distributing the intratumoral liposome distribution more uniformly, only a calculated activity of 68 MBq (1.8 mCi), on average, was modeled to give approximately 100% TCP.

IV. DISCUSSION

The effects on tumor control by the intratumoral liposome distribution following direct intratumoral infusion were investigated in this work. The results have important implications for radionuclide therapy with liposome encapsulation as well as other radionuclide therapy modalities for cancer treatment. Large heterogeneous absorbed dose distributions were shown to result in a low probability of tumor control as a consequence of low dose regions within the tumor, even though large average tumor dose levels were achieved. Using average tumor dose as a predictor of therapy response with this method of radiation delivery may overestimate the therapeutic effect, resulting in a poor clinical outcome. Mixed results seen in current clinical uses of radionuclide therapy modalities may be further evidence of the results described in this work. In the past, nonresectable pancreatic cancer patients have been treated with a direct interstitial tumor infusion technique using colloidal ^{32}P.[35] Patients received av-

TABLE III. Biological index calculations for single tumor infusion site (a), increased specific activity (b), and multiple tumor infusion sites (c).

	Tumor volume (cm^3)	Injected activity (MBq)		EUD (Gy)		TCP (%)		Average dose (Gy)	
		^{186}Re	^{188}Re	^{186}Re	^{188}Re	^{186}Re	^{188}Re	^{186}Re	^{188}Re
(a)									
Rat 1	1.57	76.96	76.96	4.64	10.17	0.00	0.00	767.81	496.12
Rat 2	1.84	92.13	92.13	4.63	9.18	0.00	0.00	588.97	399.87
Rat 3	1.28	64.75	64.75	6.55	16.58	0.00	27.85	542.43	287.41
Rat 4	0.78	37.37	37.37	6.04	27.81	0.00	98.99	360.21	274.97
Average ± SD	1.36 ± 0.46	67.80 ± 23.17	67.80 ± 23.17	5.47 ± 0.98	15.94 ± 8.57	0.00 ± 0.00	31.71 ± 46.74	564.86 ± 167.49	364.59 ± 104.14
(b)									
Rat 1	1.57	10 020.3	616.8	29.95	30.53	99.09	99.28	99 815.38	3968.92
Rat 2	1.84	15 639.5	1195.8	30.26	30.18	99.07	99.04	100 124.65	5198.29
Rat 3	1.28	5 301.0	193.9	29.40	30.03	99.10	99.29	44 479.13	862.24
Rat 4	0.78	1 268.0	37.4	28.19	27.81	99.12	98.99	12 247.07	274.971
Average ± SD	1.36 ± 0.46	8 057.2 ± 6 192.4	511.0 ± 518.0	29.45 ± 0.91	29.64 ± 1.24	99.10 ± 0.02	99.15 ± 0.16	64 166.56 ± 43 386.06	2576.11 ± 2383.86
(c)									
Rat 1	1.57	76.96	76.96	50.20	74.02	100.00	100.00	752.84	480.73
Rat 2	1.84	92.13	92.13	30.95	35.10	99.28	99.86	562.45	378.50
Rat 3	1.28	64.75	64.75	92.19	112.00	100.00	100.00	494.69	256.41
Rat 4	0.78	37.37	37.37	46.67	93.49	100.00	100.00	364.19	270.99
Average ± SD	1.36 ± 0.46	67.80 ± 23.17	67.80 ± 23.17	55.00 ± 26.17	78.65 ± 32.92	99.8 ± 0.36	99.97 ± 0.07	543.54 ± 161.98	346.66 ± 104.66

erage tumor doses from 235 to 17 000 Gy, ablative dose levels unheard of in EBRT modalities due to toxicity issues. However, median survival was only improved to 12 months compared to 8–10.4 months seen with EBRT of 60 or 35–40 Gy with concomitant 5-fluorouracil.[36] Even with the large average tumor absorbed doses, complete tumor eradication was not achieved and heterogeneous intratumoral absorbed dose distributions may be at fault.

This work described possible approaches for improving tumor control with intratumorally infused radionuclide encapsulated liposomes. Encapsulating radionuclides with higher energy beta emissions, absorbed dose escalation through increased specific activity, or obtaining a more homogeneous intratumorally infused liposomal radionuclide distribution through increasing the number of tumor injection sites was shown to increase EUD and TCP. In a clinical setting, a combination of these pathways tailored to individual patients (e.g., tumor size, tumor location, and ease of access for multiple injection sites) would be beneficial for treatment efficacy. For example, since the infused activity was dependent on the tumor volume, a ratio of the required activity to give over 99% TCP (Table IIIb) and the actual infused activity from the *in vivo* animal study (Table IIIa) increased from 33.9 and 1.0 for the smallest tumor size to 169.8 and 13.0 for the largest tumor size when injecting ^{186}Re and ^{188}Re liposomes, respectively. This indicates greater intratumoral liposome heterogeneity for larger tumor sizes and likely requiring multiple tumor injection locations in a clinical setting in order to have complete tumor control while keeping the required amount of injected activity at moderate levels. Dose escalation for tumors modeled with infused ^{186}Re liposomes required much more activity to be injected due to greater intratumoral absorbed dose heterogeneity and the fact that EUD and TCP, unlike absorbed dose, are not linearly related to cumulative activity. This can potentially lead to toxicity issues within organs with abundant liposomal uptake within the reticuloendothelial system.[11] Encapsulated radionuclides with higher energy beta emissions would also be beneficial for larger tumors as the locoregional treatment range is defined by this energy. The more penetrating beta emissions from ^{188}Re were shown to have better tumor absorbed dose coverage compared to ^{186}Re, even with a higher average tumor doses per injected activity from ^{186}Re liposomes.

In this study, it was modeled to be more efficient, in terms of required activity for tumor control, to increase the number of tumor injection sites to distribute the liposomes more homogeneously within the tumor. It is conceivable to use image guidance with combined SPECT/CT or other imaging modalities, which coregister detailed anatomical information with activity distributions for multiple injection locations. Following the first tumor infusion, a hybrid imaging modality may be used to guide the placement of the next injection to a tumor region with low activity deposition. An alternative option would be to just assume that increasing the number of tumor infusion sites, although more time consuming in a clinical setting, will distribute the infused liposomal radionuclides more uniformly within the tumor. Although the image guidance delivery to regions of low liposome uptake may not be a requirement, therapy outcome predictability may be less accurate as there would still be possible low dose regions within the tumor. This latter technique has previously been

used with human HNSCC xenografts in nude rats receiving direct intratumoral injections of radionuclide encapsulated liposomes.[11] Exceptional tumor control was achieved with low levels of infused ^{186}Re-liposome activity concentrations with the use of three tumor infusion sites. The low activity concentrations used along with the level of tumor control seen validate the use of multiple infusion locations for therapy effectiveness, even for the less energetic ^{186}Re emissions. Although this work considered head and neck cancer, this technique could be extended to the majority of tumor locations with the use of a practical image guidance delivery system, such as the use of CT for image-guided infusion to nonresectable pancreatic cancer or ultrasound guidance for intratumoral injection to breast lesions.[35,37]

V. CONCLUSIONS

This work provided important considerations for cancer therapy using direct intratumorally infused radionuclide encapsulated liposomes. Common dosimetric and radiobiological indices were used with *in vivo* small animal SPECT/CT imaging to assess how the intratumoral absorbed dose distribution of intratumorally infused radionuclide encapsulated liposomes could affect cancer therapy. Increased beta emission energy, increased radionuclide specific activity, as well as the use of multiple tumor infusion sites were shown to improve calculated EUD and TCP values; however, the modeling of multiple injection locations indicated that the resulting more homogeneous intratumoral liposome distributions to be most efficient in terms of activity usage for achieving nearly 100% TCP. The use of average tumor doses was shown to be insufficient in providing a relationship between treatment and effect, and the resulting intratumoral distribution of liposomes following infusion should be taken into account in treatment planning and evaluation.

ACKNOWLEDGMENTS

This study was supported by the National Cancer Institute (NCI) Grant No. R01 CA131039. One of the authors (Brian A. Hrycushko) was supported by the National Institute of Biomedical Imaging and Bioengineering (NIBIB) Training Grant No. T-32 EB000817.

[a]Electronic mail: bao@uthscsa.edu

[1]D. J. Simpkin and T. R. Mackie, "EGS4 Monte Carlo determination of the beta dose kernel in water," Med. Phys. **17**, 179–186 (1990).
[2]E. Mainegra-Hing, D. W. Rogers, and I. Kawrakow, "Calculation of photon energy deposition kernels and electron dose point kernels in water," Med. Phys. **32**, 685–699 (2005).
[3]W. V. Prestwich, J. Nunes, and C. S. Kwok, "Beta dose point kernels for radionuclides of potential use in radioimmunotherapy," J. Nucl. Med. **30**, 1036–1046 (1989).
[4]B. A. Hrycushko, S. Li, C. Shi, B. Goins, Y. Liu, W. T. Phillips, P. M. Otto, and A. Bao, "Postlumpectomy focal brachytherapy for simultaneous treatment of surgical cavity and draining lymph nodes," Int. J. Radiat. Oncol., Biol., Phys. **79**, 948–955 (2010).
[5]D. M. Goldenberg, "Targeted therapy of cancer with radiolabeled antibodies," J. Nucl. Med. **43**, 693–713 (2002).
[6]S. H. Britz-Cunningham and S. J. Adelstein, "Molecular targeting with radionuclides: State of the science," J. Nucl. Med. **44**, 1945–1961 (2003).
[7]J. Zheng, D. Jaffray, and C. Allen, "Quantitative CT imaging of the spatial and temporal distribution of liposomes in a rabbit tumor model," Mol. Pharmacol. **6**, 571–580 (2009).
[8]A. Bao, W. T. Phillips, B. Goins, X. Zheng, S. Sabour, M. Natarajan, F. R. Woolley, C. Zavaleta, and R. A. Otto, "Potential use of drug carried-liposomes for cancer therapy via direct intratumoral injection," Int. J. Pharm. **316**, 162–169 (2006).
[9]A. A. Gabizon, "Applications of liposomal drug delivery systems to cancer therapy," in *Nanotechnology for Cancer Therapy*, edited by M. M. Amiji (CRC, Boca Raton, 2007), pp. 595–611.
[10]D. Emfietzoglou, K. Kostarelos, and G. Sgouros, "An analytical dosimetry study for the use of radionuclide-liposome conjugates in internal radiotherapy," J. Nucl. Med. **42**, 499–504 (2001).
[11]J. T. French, B. Goins, M. Saenz, S. Li, X. Garcia-Rojas, W. T. Phillips, R. A. Otto, and A. Bao, "Interventional therapy of head and neck cancer with lipid nanoparticle-carried rhenium-186 radionuclide," J. Vasc. Interv. Radiol. **21**, 1271–1279 (2010).
[12]A. Bao, B. Goins, R. Klipper, G. Negrete, M. Mahindaratne, and W. T. Phillips, "A novel liposome radiolabeling method using ^{99m}Tc-"SNS/S" complexes: In vitro and in vivo evaluation," J. Pharm. Sci. **92**, 1893–1904 (2003).
[13]A. Bao, B. Goins, R. Klipper, G. Negrete, and W. T. Phillips, "^{186}Re-liposome labeling using ^{186}Re-SNS/S complexes: In vitro stability, imaging, and biodistribution in rats," J. Nucl. Med. **44**, 1992–1999 (2003).
[14]S. X. Wang, A. Bao, S. J. Herrera, W. T. Phillips, B. Goins, C. Santoyo, F. R. Miller, and R. A. Otto, "Intraoperative ^{186}Re-liposome radionuclide therapy in a head and neck squamous cell carcinoma xenograft positive surgical margin model," Clin. Cancer Res. **14**, 3975–3983 (2008).
[15]S. X. Wang, A. Bao, W. T. Phillips, B. Goins, S. J. Herrera, C. Santoyo, F. R. Miller, and R. A. Otto, "Intraoperative therapy with liposomal drug delivery: Retention and distribution in human head and neck squamous cell carcinoma xenograft model," Int. J. Pharm. **373**, 156–164 (2009).
[16]A. Syme, S. McQuarrie, and B. G. Fallone, "Beta dose-rate distributions in microscopic spherical tumors for intraperitoneal radioimmunotherapy," Int. J. Radiat. Oncol., Biol., Phys. **56**, 1495–1506 (2003).
[17]A. Bao, W. T. Phillips, B. Goins, H. S. McGugg, X. Zheng, F. R. Woolley, M. Natarajan, C. Santoyo, F. R. Miller, and R. A. Otto, "Setup and characterization of a human head and neck squamous cell carcinoma xenograft model in nude rats," Otolaryngol.-Head Neck Surg. **135**, 853–857 (2006).
[18]M. M. Tomayko and C. P. Reynolds, "Determination of subcutaneous tumor size in athymic (nude) mice," Cancer Chemother. Pharmacol. **24**, 148–154 (1989).
[19]G. Sgouros, S. Squeri, A. M. Ballangrud, K. S. Kolbert, J. B. Teitcher, K. S. Panageas, R. D. Finn, C. R. Divgi, S. M. Larson, and A. D. Zelenetz, "Patient-specific, 3-dimensional dosimetry in non-Hodgkin's lymphoma patients treated with ^{131}I-anti-B1 antibody: Assessment of tumor dose-response," J. Nucl. Med. **44**, 260–268 (2003).
[20]A. R. Prideaux, H. Song, R. F. Hobbs, B. He, E. C. Frey, P. W. Ladenson, R. L. Wahl, and G. Sgouros, "Three-dimensional radiobiologic dosimetry: Application of radiobiological modeling to patient-specific 3-dimensional imaging-based internal dosimetry," J. Nucl. Med. **48**, 1008–1016 (2007).
[21]G. Sgouros, K. S. Kolbert, A. Sheikh, K. S. Pentlow, E. F. Mun, A. Barth, R. J. Robbins, and S. M. Larson, "Patient-specific dosimetry for ^{131}I thyroid cancer therapy using ^{124}I PET and 3-dimensional-internal dosimetry (3D-ID)," J. Nucl. Med. **45**, 1366–1372 (2004).
[22]H. B. Giap, D. J. Macey, J. E. Bayouth, and A. L. Boyer, "Validation of a dose-point kernel convolution technique for internal dosimetry," Phys. Med. Biol. **40**, 365–381 (1995).
[23]A. Bao, X. Zhao, W. T. Phillips, F. R. Woolley, R. A. Otto, B. Goins, and J. M. Hevezi, "Theoretical study of the influence of a heterogeneous activity distribution on intratumoral absorbed dose distribution," Med. Phys. **32**, 200–208 (2005).
[24]I. Kawrakow and D. W. Rogers, "The EGSnrc code system: Monte Carlo simulation of electron and photon transport," Technical Report No. PIRS-701 (National Research Council of Canada, Ottawa, Canada, 2000).
[25]D. W. Rogers, I. Kawrakow, J. P. Seuntjens, B. R. B. Walters, and E. Mainegra-Hing, "NRC user codes for EGSnrc," Technical Report No. PIRS-702 (National Research Council of Canada, Ottawa, Canada, 2003).
[26]M. G. Stabin and L. da Luz, "Decay data for internal and external dose assessment," Health Phys. **83**, 471–475 (2002).
[27]Data produced using the MIRD program and extracted from the Evaluated Nuclear Structure Data File (ENSDF) (December 15, 2008). Additional calculations performed by the program RADLST. T. W. Burrows,

"The program RADLST," Report No. BNL-NCS-52142.(National Nuclear Data Center, Brookhaven National Laboratory, USA, 1988).
[28]A. Niemierko, "Reporting and analyzing dose distributions: A concept of equivalent uniform dose," Med. Phys. **24**, 103–110 (1997).
[29]W. M. Butler, R. R. Stewart, and G. S. Merrick, "A detailed radiobiologic and dosimetric analysis of biochemical outcomes in a case-control study of permanent prostate brachytherapy patients," Med. Phys. **36**, 776–787 (2009).
[30]S. Webb and A. E. Nahum, "A model for calculating tumour control probability in radiotherapy including the effects of inhomogeneous distributions of dose and clonogenic cell density," Phys. Med. Biol. **38**, 653–666 (1993).
[31]S. M. Bentzen, "Steepness of the clinical dose-control curve and variation in the in vitro radiosensitivity of head and neck squamous cell carcinoma," Int. J. Radiat. Biol. **61**, 417–423 (1992).
[32]B. Maciejewski, H. R. Withers, J. M. Taylor, and A. Hliniak, "Dose fractionation and regeneration in radiotherapy for cancer of the oral cavity and oropharynx: Tumor dose-response and repopulation," Int. J. Radiat. Oncol., Biol., Phys. **16**, 831–843 (1989).
[33]H. R. Withers, "Radiation biology and treatment options in radiation oncology," Cancer Res. **59**, 1676s–1684s (1999).
[34]S. M. Bentzen, A. C. Ruifrok, and H. D. Thames, "Repair capacity and kinetics for human mucosa and epithelial tumors in the head and neck: Clinical data on the effect of changing the time interval between multiple fractions per day in radiotherapy," Radiother. Oncol. **38**, 89–101 (1996).
[35]S. E. Order, J. A. Siegel, R. Principato, L. E. Zeiger, E. Johnson, P. Lang, R. Lustig, and P. E. Wallner, "Selective tumor irradiation by infusional brachytherapy in nonresectable pancreatic cancer: A phase I study," Int. J. Radiat. Oncol., Biol., Phys. **36**, 1117–1126 (1996).
[36]A. S. DeNittis, M. D. Stambaugh, P. Lang, P. E. Wallner, R. A. Lustig, R. O. Dillman, and S. E. Order, "Complete remission of nonresectable pancreatic cancer after infusional colloidal phosphorus-32 brachytherapy, external beam radiation therapy, and 5-fluorouracil: A preliminary report," Am. J. Clin. Oncol. **22**, 355–360 (1999).
[37]S. H. Estourgie, O. E. Nieweg, R. A. Valdez Olmos, E. J. Th. Rutgers, and B. B. Kroon, "Intratumoral versus intraparenchymal injection technique for lymphoscintigraphy in breast cancer," Clin. Nucl. Med. **28**, 371–374 (2003).